Macromolecules
ARTICLE

Macromolecules **2010**, *43*, 4943–4953 **4943**
DOI: 10.1021/ma1004265

Self-Assembled Polymeric Nanoparticles of Organocatalytic Copolymerizated D,L-Lactide and 2-Methyl 2-Carboxytrimethylene Carbonate

Jiao Lu[†] and Molly S. Shoichet*[,†,‡,§]

[†]*Department of Chemistry,* [‡]*Department of Chemical Engineering and Applied Chemistry, and* [§]*Institute for Biomaterials and Biomedical Engineering, Terrence Donnelly Center for Cellular and Biomolecular Research, University of Toronto, 160 College Street Room 514, Toronto, ON M5S 3E1*

Received February 26, 2010; Revised Manuscript Received April 14, 2010

ABSTRACT: Polymeric nanoparticles are important for the selective delivery of hydrophobic cancer drugs to tumors, yet most of the polymers studied are limited by compositional diversity. To overcome this limitation, a series of poly(D,L-lactide-*co*-2-methyl-2-carboxytrimethylene carbonate) (P(LA-*co*-TMCC)) was synthesized with low polydispersity index (PDI: 1.25 to 1.36) using organocatalytic ring-opening copolymerization with pyrenebutanol initiation and 1-[3,5-bis(trifluoromethyl) phenyl]-3-[(1*R*,2*R*)-(−)-2-(dimethylamino) cyclohexyl] thiourea (thiourea-amine) catalysis. The reactivity ratio was estimated at 1.1 for LA and 0.072 for benzyl-protected TMCC. We controlled the copolymer molar mass and composition by varying monomer-to-initiator ratios and monomer feed ratios. Methoxy-terminated poly(ethylene glycol) amine (MeO-PEG-NH_2) was coupled to the carboxylic acid groups of the TMCC copolymer backbone using carbodiimide chemistry. The resulting amphiphilic copolymer self-assembled in aqueous solution to form nanoparticles with a narrow size distribution. Smaller nanoparticles formed when borate buffer (vs water) were present during the self-assembly process. The physical properties of the nanoparticles, such as size, critical micelle concentration (CMC), and ζ potential were affected by the hydrophilic PEG chain length and the hydrophobic backbone composition. Those nanoparticles with the lowest CMC are thought to be sufficiently stable for targeted delivery in cancer.

Introduction

Polymeric nanoparticles are particularly interesting for the selective delivery of hydrophobic anticancer drugs to tumor tissues because their size takes advantage of the enhanced permeability and retention effect,[1] resulting in improved pharmacological and therapeutic properties of many anticancer drugs.[2,3] Most polymeric nanoparticles are amphiphilic, having a hydrophobic core that promotes the solubility of hydrophobic drugs and a hydrophilic shell that allows for longer blood circulation. Encapsulation or conjugation of clinically approved drugs into nanoscale delivery vehicles allows for greater tissue targeting and reduced systemic toxicity in cancer therapy, thereby overcoming the poor biodistribution and systemic toxicity associated with most anticancer drugs.

The majority of amphiphilic polymers used in drug delivery are composed of block copolymers of hydrophilic poly(ethylene glycol) and hydrophobic polymers such as aliphatic polyesters and polycarbonates including: poly(lactic acid) (PLA), poly(glycolic acid) (PGA), their copolymers (PLGA), poly(caprolactone) (PCL), and poly(trimethylene carbonate) (PTMC).[4−7] These polymers are most commonly synthesized by ring-opening polymerization (ROP) of cyclic esters or carbonates, where coordination−insertion, cationic, anionic, and nucleophilic polymerization routes have been described.[8] The classic coordination/insertion mechanism primarily involves electrophilic activation of the monomer by Lewis acids, which contain metals such as Sn (II);[8,9] however, in the presence of Sn (II), most polymerizations of cyclic esters result in broad polymer molar mass distributions.[10−13] Moreover, residual tin is difficult to completely remove, and this can lead to undesirable toxicity and inflammation in vivo.

Organocatalysis provides an excellent alternative to transition-metal catalysis of cyclic esters and carbonates because it avoids the use of metals and provides better control over the polymerization reaction, resulting in near monodisperse polymers. The chiral bifunctional organic catalyst containing thiourea and tertiary amino group **4** (Scheme 1) effectively activates nitro compounds for enantioselective aza-Henry reaction and Michael addition.[14−16] Recently, Hedrick et al.[17] used this bifunctional organocatalyst for solution ROP of lactide, which resulted in PLA with a narrow polydispersity index (PDI) < 1.08. The molar mass of PLA was controlled by varying the monomer-to-initiator ratio.[17] Whereas the rate of reaction was slow, with complete conversion requiring up to 105 h, broadening of PDI was not observed, indicating that little transesterification of the linear polymer occurred. Importantly, polymer molar mass increased with the addition of more monomer, demonstrating that this was a living polymerization.

We were interested in synthesizing poly(D,L-lactide-*co*-2-methyl-2-carboxytrimethylene carbonate) (P(LA-*co*-TMCC)) because the carboxylate group can be used to graft amine-terminated poly(ethylene glycol)-methoxy (MeO-PEG-NH_2).[13,18] These amphiphilic P(LA-*co*-TMCC)-*g*-PEG self-assemble to nanoparticles that are compelling for targeted drug delivery in cancer because of their resulting nanoparticle size and low CMC.[13,19] By coupling PEG-furan or PEG-azide (instead of PEG-methoxy), these polymeric nanoparticles were surface-modified by aqueous "click" chemistry, using Diels−Alder or Huisgen 1,3-cylcoaddition chemistry, respectively, to immobilize Herceptin[13] or arginine-glycine-aspartic acid (RGD) peptides.[19] In these studies, Herceptin-modified

*To whom correspondence should be addressed. Tel: 416-978-1460. Fax: 416-978-4317. E-mail: molly.shoichet@utoronto.ca.

Published on Web 05/04/2010

Scheme 1. Synthesis of P(TMCC-*co*-LA)-*g*-PEG by Living, Ring-Opening Polymerization

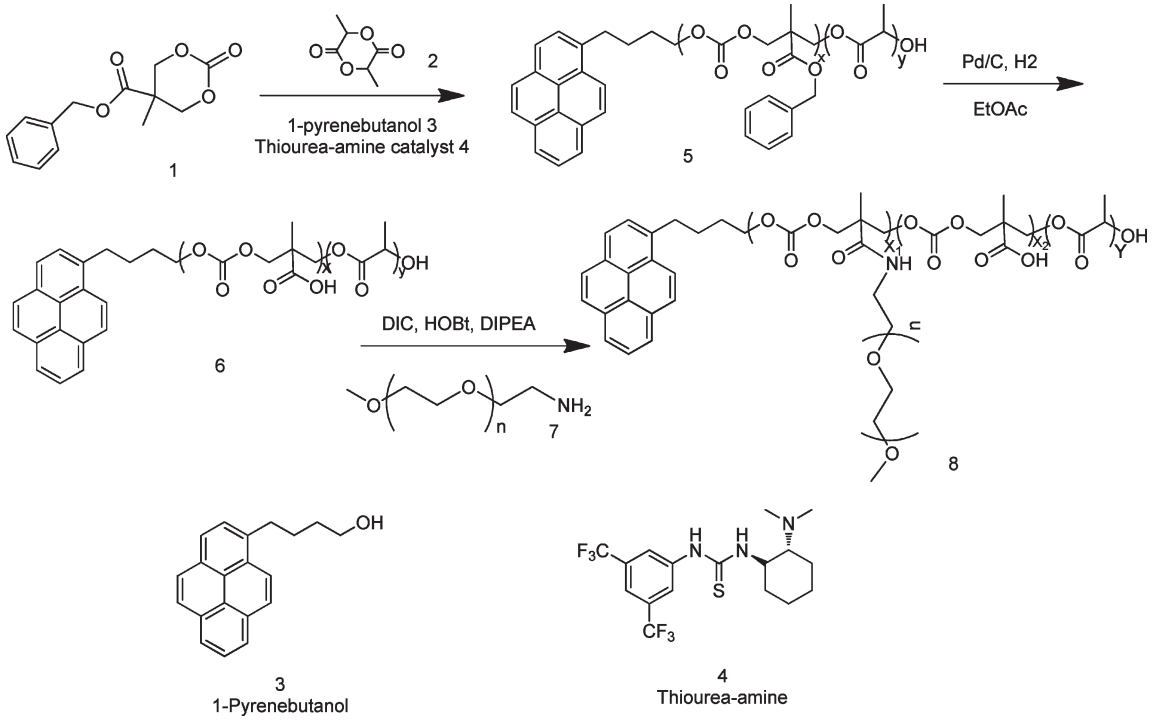

nanoparticles bound specifically to HER2+ breast cancer cells, whereas RGD peptide-modified nanoparticles bound specifically to rabbit corneal epithelial cells. Notwithstanding these important results, the bulk polymerization of TMCC and LA, results in polydisperse polymers, and the resulting nanoparticles have a broad size distribution.

We hypothesized that the thiourea amine organocatalyst **3** with pyrene butanol **4** initiation (Scheme 1) could be used to synthesize near monodisperse P(LA-*co*-TMCC) with a range of copolymer compositions. Moreover, we hypothesized that these near monodisperse P(LA-*co*-TMCC)-*g*-PEG would self-assemble to nanoparticles with a narrower size distribution than similarly self-assembled polydisperse P(LA-*co*-TMCC)-*g*-PEG. Using the dialysis method of self-assembly, polymers are dissolved in an organic solvent and then dialyzed against water. During this process, the hydrophobic chains associate by hydrophobic interactions, and those chains with longer hydrophobic blocks self-assemble to form micelles first, followed by polymer chains with shorter hydrophobic blocks. For a polydisperse sample, we expect this to result in a broad population distribution of nanoparticles, whereas for a near monodisperse polymer, we anticipate a narrow population distribution of nanoparticles.[20]

To test these hypotheses, we synthesized a series of P(LA-*co*-TMCC) where the LA-to-TMCC monomer ratio was varied. The polymers were characterized for molar mass and PDI. PEG, of varying molar mass, was grafted to the P(LA-*co*-TMCC) backbone, resulting in an amphiphilic polymer that self-assembled in water to nanoparticles. The presence of carboxylate groups of TMCC allowed us to manipulate the self-assembly process with pH. By varying the molar mass of PEG, the impact of hydrophobic to hydrophilic segments on the size, ζ potential, and critical micelle concentration (CMC) of self-assembled particles were also studied.

Experimental Section

Materials. All solvents and reagents were purchased from Sigma-Aldrich and used as received, unless otherwise noted. Methoxy-terminated poly(ethylene glycol) amine 10K (MeO-PEG-NH_2 10K) was obtained from Rapp Polymer (Germany), and the thiourea-amine catalyst, 1-[3,5-bis(trifluoromethyl)phenyl]-3-[(1*R*,2*R*)-(−)-2(dimethylamino) cyclohexyl] thiourea (*R*,*R*-TUC), was obtained from Strem Chemicals (Newburyport, MA). The synthesis of 5-methyl-5-benzyloxycarbonyl-1,3-trimethylene carbonate (benzyl-protected TMCC, TMCC-Bn) has been previously reported.[13] TMCC-Bn and D,L-lactide monomers were purified by precipitation in toluene. Thiourea-amine and pyrenebutanol were dried over calcium hydride in freshly distilled dichloromethane before use. All glassware was flame-dried under vacuum before use. Dialysis membrane (no. 132109) with a molecular weight cut off (MWCO) of 2 kDa was purchased from Spectrum Laboratories Rancho Dominguex (Rancho Dominguex, CA). All dialysis was carried out in 4 L of distilled water. The water was changed every 2 h for the first 8 h and then left overnight.

Borate buffer solution preparation: The pH of the borate buffer was manipulated to control the self-assembly process of P(LA-*co*-TMCC)-*g*-PEG. Boric acid (3.1 g, 0.05 mol, 62 g/mol) dissolved in 100 mL of distilled water results in a pH 5 solution, which was used for polymer self-assembly at acidic pH. To achieve a buffered solution at pH 7 and 9, 10 N NaOH was added dropwise to the boric acid solution.

Instruments. The ^{1}H NMR spectra were recorded in either $CDCl_3$ or DMSO-d_6 solvent using a Varian Auto X8308-400 spectrometer. Molar mass and PDI of P(LA-*co*-TMCC-Bn) were measured by gel permeation chromatography (GPC) in THF relative to polystyrene standards on a system equipped with two-column (Viscoteck GMHhr-M and Viscoteck GMHhr-H) and triple detector array (TDA302) at room temperature with a flow rate of 0.6 mL/min THF mobile phase. The CMC was measured using surface tension measurements with a Wilhelmy plate and a Sigma 700 tensiometer (KVS Instrument, Ltd.). Particle solutions in 10 mM PBS (pH 7.4) at concentration ranges from 0.1 to 300 μg/mL were prepared. The disposable VWR microcover glass (22 × 50 mm) was used for each measurement at room temperature. Measurement of the reading force was taken after 300 s, and the surface tension measurements were plotted against the logarithm of copolymer concentration. The CMC was determined from the intersection of two

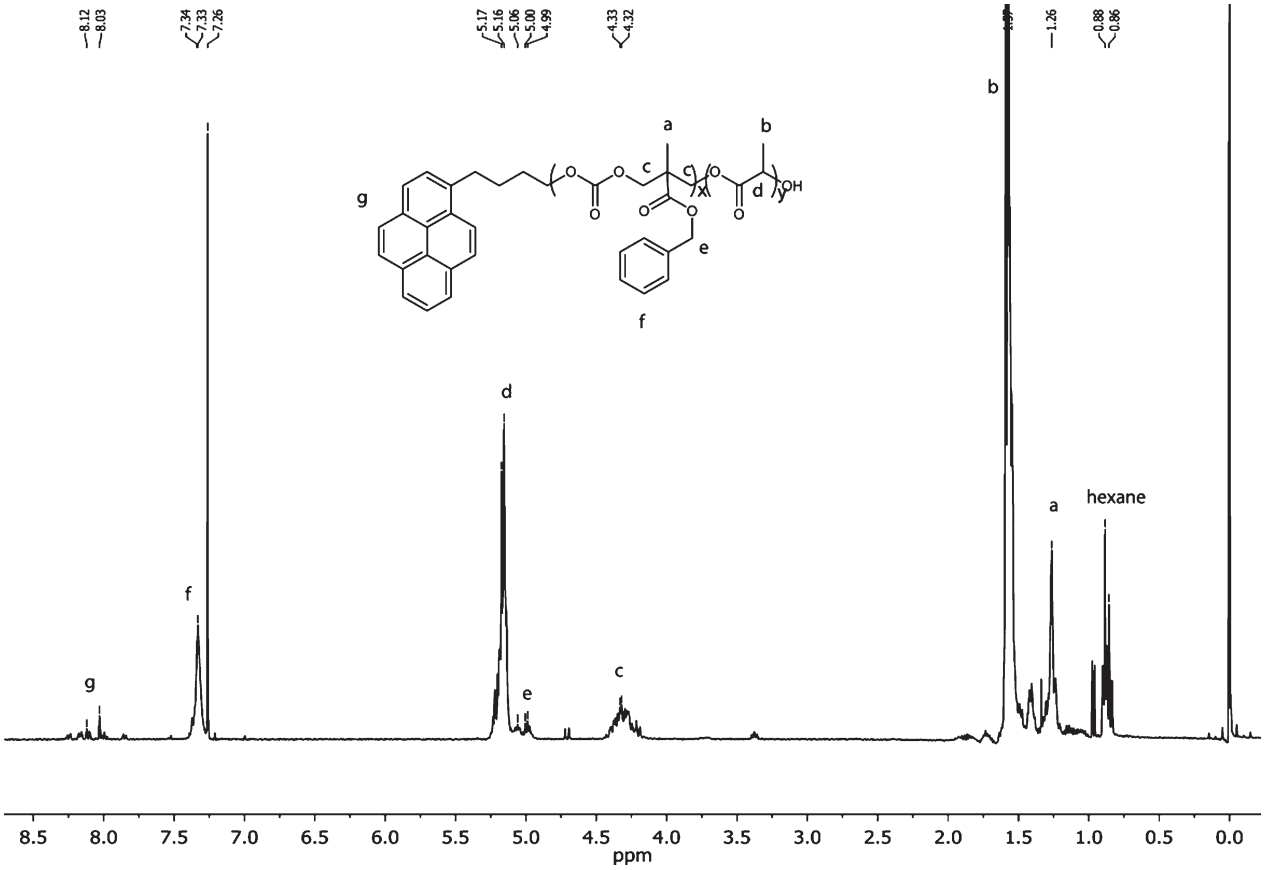

Figure 1. ^{1}H NMR spectrum P(LA-*co*-TMCC-Bn). ^{1}H NMR($CDCl_3$): δ 1.27 (m, CH_3 from TMCC), 1.57−1.59 (m, CH_3 from LA), 4.32 (m, CH_2 from TMCC), 4.99 (m, methylene), 5.00−5.19 (m, CH from LA), 7.34 (s, benzyl group), and 7.78−8.25 (m, conjugated pyrene).

straight lines, one in the descending part of the curve and the other through the plateau. Nanoparticle size was measured by a Malvern Zetasizer Nano ZS, which is equipped with a 4 mW, 633 nm laser. During the measurement, samples were held in polystyrene cuvettes (Küvetten, Germany). The average is reported of three individual samples, prepared under the same conditions, with 12 runs each. All samples have a concentration of ~1 mg/mL and were filtered through NY-0.45 μm filter (Progene, QC, Canada) before measurement. ζ potential was measured under the same conditions using folded capillary cells (Malvern, DTS 1060). The TEM images were obtained with a Hitachi H-7000 conventional transmission electron microscope operated at 75 kV. We prepared samples by placing one drop of particle solution at a concentration of ~0.4 mg/mL in distilled water on a 300 mesh Formvar/carbon-film-coated copper grid Electron Microscopy Sciences (Fort Washington, PA). The solvent was allowed to evaporate at room temperature in the fume hood prior to imaging.

Methods. *Synthesis of P(LA-co-TMCC-Bn) ([M]:[I] = 50, 10% TMCC) **5***. A 25 mL round-bottomed flask with a stir bar and several molecular sieves (4 Å) within was oven-dried overnight and flame-dried under vacuum before use. 3,6-Dimethyl-1,4-dioxane-2,5-dione **2** (1.5 g, 10.4 mmol, each monomer contains two repeating units), 5-methyl-5-benzyloxycarbonyl-1,3-trimethylene carbonate **1** (0.58 g, 2.3 mmol), *R,R*-TUC (0.14 g, 0.35 mmol), and pyrenebutanol (70 mg, 0.25 mmol) were dissolved in freshly distilled CH_2Cl_2 (10 mL) in a round-bottomed flask and sealed with rubber septum under Argon. After stirring for 7 days at room temperature, the flask was vented to air, and the solution was precipitated in hexane: 5 mL of solution was precipitated in 40 mL of hexane. The precipitate was dried in the vacuum oven at room temperature for 8 h, yielding a white solid **5** (2.1 g, 98%). The crude product was then dissolved in a small amount of dichloromethane and purified through a silica column (Silia Flash P60, Silicycle, QC, Canada) with a solvent mixture of 3% CH_3OH and 0.5% NH_4OH in CH_2Cl_2. The collected fractions were dried by rotary evaporation, dissolved in 10 mL of chloroform and precipitated again in 80 mL of hexane, yielding 1.8 g (84%) of P(LA-*co*-TMCC-Bn). ^{1}H NMR ($CDCl_3$): δ 1.27 (m, CH_3 from TMCC), 1.57−1.59 (m, CH_3 from LA), 4.32 (m, CH_2 from TMCC), 4.99 (m, methylene), 5.00−5.19 (m, CH from LA), 7.34 (s, benzyl group, TMCC), and 7.78−8.25 (m, conjugated pyrene, initiator) (Figure 1).

*Deprotection of P(LA-co-TMCC-Bn) ([M]:[I] = 50, 10% TMCC) **6***. Prior to deprotection of the benzyl ester, the thiourea organocatalyst had to be completely removed because thiourea poisons metal catalysts, such as Pd, by irreversibly adsorbing at their active center.[21] The thiourea was effectively separated from the benzyl-protected P(LA-*co*-TMCC-Bn) by column chromatography prior to the hydrogenation reaction. In a 250 mL round-bottomed flask, P(LA-*co*-TMCC-Bn) **5** (1.8 g) was dissolved in 50 mL of ethylacetate, and activated palladium on carbon (225 mg, 12.5 wt % of the copolymer) was added. The flask was purged with nitrogen gas for 10 min and then with hydrogen gas for another 15 min. The reaction mixture was allowed to stir under a hydrogen balloon at 1 atm for 5 days. The hydrogen balloon was refilled every day. The Pd/C catalyst was removed by centrifugation and filtration through an NY-0.2 μm syringe filter. The filtrate was dried by rotary evaporation, dissolved in 10 mL of dichloromethane, and precipitated in 80 mL of hexane to yield 1.4 g (92%) of white solid P(LA-*co*-TMCC) **6**. The success of the benzyl deprotection reaction can be verified by the disappearance of the peak at 7.34 ppm on ^{1}H NMR spectrum (Figure 2). ^{1}H NMR ($CDCl_3$): δ 1.29 (m, CH_3 from TMCC), 1.57−1.59 (m, CH_3 from LA), 4.32 (m, CH_2 from TMCC), 5.00−5.17 (m, CH from LA). The pyrene initiating group (m, CH at 7.78−8.25) was reduced during the hydrogenation step.

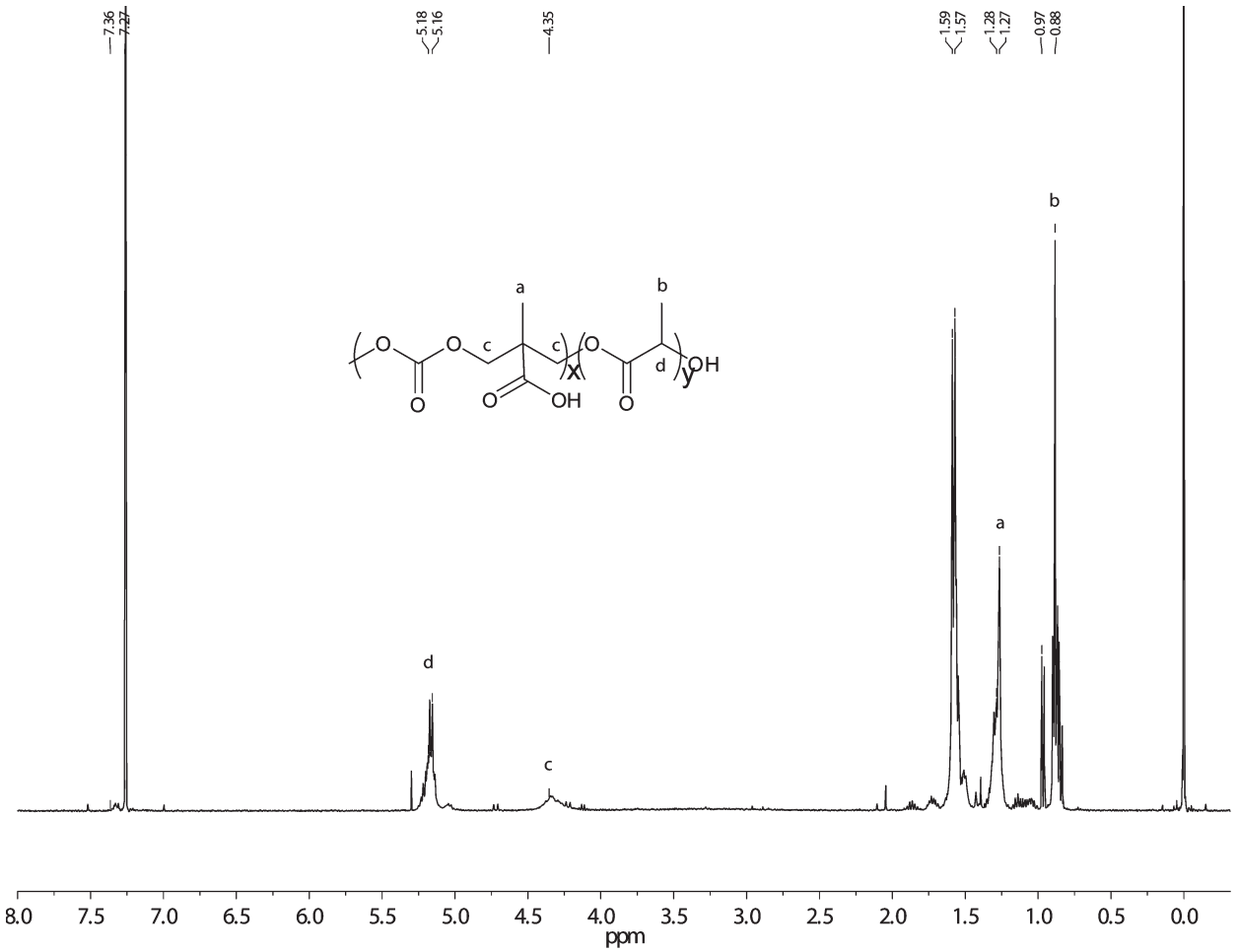

Figure 2. ^{1}H NMR spectrum of P(LA-*co*-TMCC) after benzyl deprotection. ^{1}H NMR ($CDCl_3$): δ 1.29 (m, CH_3 from TMCC), 1.57−1.59 (m, CH_3 from LA), 4.32 (m, CH_2 from TMCC), 5.00−5.17 (m, CH from LA).

Synthesis of P(LA-co-TMCC)-g-PEG ([*M*]:[*I*] = *50, 10% TMCC*) *8*. Copolymer **6** (7k, 100 mg) was first dissolved in DMF (3 mL), and then *N*,*N*′-diisopropyl-carbodiimide (DIC, 100 μL, 0.65 mmol), *N*,*N*′-diisopropylethylamine (DIPEA, 90 μL, 0.52 mmol), and hydroxybenzotriazole (HOBt, 64 mg, 0.48 mmol) were added, and the reaction solution was stirred at room temperature for 30 min. MeO-PEG-NH_2 **7** (5k, 200 mg) was dissolved in 3 mL of DMF and then added to the activated copolymer solution under Ar with additional DIPEA (90 μL, 0.52 mmol). The reaction mixture was stirred at room temperature for 48 h, after which 400 μL of borate buffer (pH 9, 500 mM) was added dropwise, and the solution was dialyzed against distilled water. The polymer solution in the dialysis bag became clear overnight. The excess PEG was removed using a Sepharose CL-6B column equilibrated with distilled water. When PEG 10K was grafted, the identical experiment was done except that the Sepharose CL-4B column was used instead because it gives better separation for higher molecular weight. The collected fractions containing polymers were freeze-dried to give a white solid **8** (55 mg, 50% yield). For 20 or 30% TMCC polymer, the quantity of DIC and HOBt was doubled, and that of DIPEA was increased by 1.5 times. ^{1}H NMR ($CDCl_3$): δ 1.23 (m, CH_3 from TMCC), 1.57−1.59 (m, CH_3 from LA), 3.64 (bs, PEG), 4.34 (m, methylene from TMCC), and 5.16 (m, CH from LA).

Reactivity Ratio Study of LA and TMCC-Bn. The monomer reactivity ratios were calculated at low conversion (< 10%) from the copolymer composition at various monomer feed ratios using the error in variables model (EVM) method[22] and the computer software package reactivity ratios error in variable model (RREVM).[23] The RREVM computer program accounts for errors in all variables, including errors in measuring the feed composition, *f*, and copolymer composition, *F*. The error was estimated to be 5% in the initial monomer feed composition based on mass measurement and 10% for the copolymer composition based on ^{1}H NMR peak area analysis. We calculated the reactivity ratios by using the Mayo−Lewis instantaneous copolymer composition eq 1

$$\frac{F_{\mathrm{LA}}}{F_{\mathrm{TMCC\text{-}Bn}}} = \frac{(r_{\mathrm{LA}}[\mathrm{M_{LA}}] + [\mathrm{M_{TMCC\text{-}Bn}}])[\mathrm{M_{LA}}]}{(r_{\mathrm{TMCC\text{-}Bn}}[\mathrm{M_{TMCC\text{-}Bn}}] + [\mathrm{M_{LA}}])[\mathrm{M_{TMCC\text{-}Bn}}]} \quad (1)$$

where F_{LA} and $F_{\mathrm{TMCC\text{-}Bn}}$ are the mole fractions of monomers LA and TMCC-Bn that are incorporated into the copolymer at instant time; r_{LA} and $r_{\mathrm{TMCC\text{-}Bn}}$ are reactivity ratio values; and $[\mathrm{M_{LA}}]$ and $[\mathrm{M_{TMCC\text{-}Bn}}]$ are the molar feed ratios of monomers LA and TMCC-Bn. This method requires initial estimation of reactivity ratios r_{LA} and $r_{\mathrm{TMCC\text{-}Bn}}$. The reactivity ratios from Jie[24] were chosen as starting values: $r_{\mathrm{LA}} = 1.03$ and $r_{\mathrm{TMC}} = 0.76$.

Copolymer Self-Assembly in Water. P(LA-*co*-TMCC)-*g*-PEG (4 mg) was dissolved in 1.0 mL of DMF, and then 0.5 mL of distilled water was added dropwise to the stirred solution at a rate of ~1 drop per 3 s. The resulting colloidal solution was placed in a dialysis bag and dialyzed against distilled water to remove the DMF for 24 h.

Copolymer Self-Assembly at pH 5, 7, and 9 with 16 mM Borate Buffer. P(LA-*co*-TMCC)-*g*-PEG (4 mg) was dissolved in 1.0 mL of DMF, and then 50 μL of borate buffer (pH 5, 7 or 9, 500 mM) was added. As the addition of buffer progressed, the quality of the solvent for the backbone decreased gradually. To ensure clarity of the solution, 0.5 mL (or 35 wt %) of water was slowly

Table 1. Characterization of P(LA-*co*-TMCC-Bn) by GPC and ^{1}H NMR

TMCC-Bn in feed (mol %)	[M]:[I]	conversion (%)	M_n (GPC)	PDI	M_n (^{1}H NMR)	DP TMCC[a]	DP LA[a]	TMCC-Bn in copolymer (mol %)
10[b]	50:1	99	6200	1.25	7400	7	77	8.3[c]
10[d]	100:1	97	11 800	1.34	12 000	12	120	9.1[c]
20[e]	100:1	95	6600	1.36	8400	15	60	20
30[e]	100:1	95	6900	1.35	9100	23	43	35

[a] Degree of polymerization was estimated based on ^{1}H NMR. [b] Reaction time: t = 7 days. [c] Referred to as 10 mol % of TMCC in copolymer. [d] Reaction time: t = 8 days. [e] Reaction time: t = 12 days.

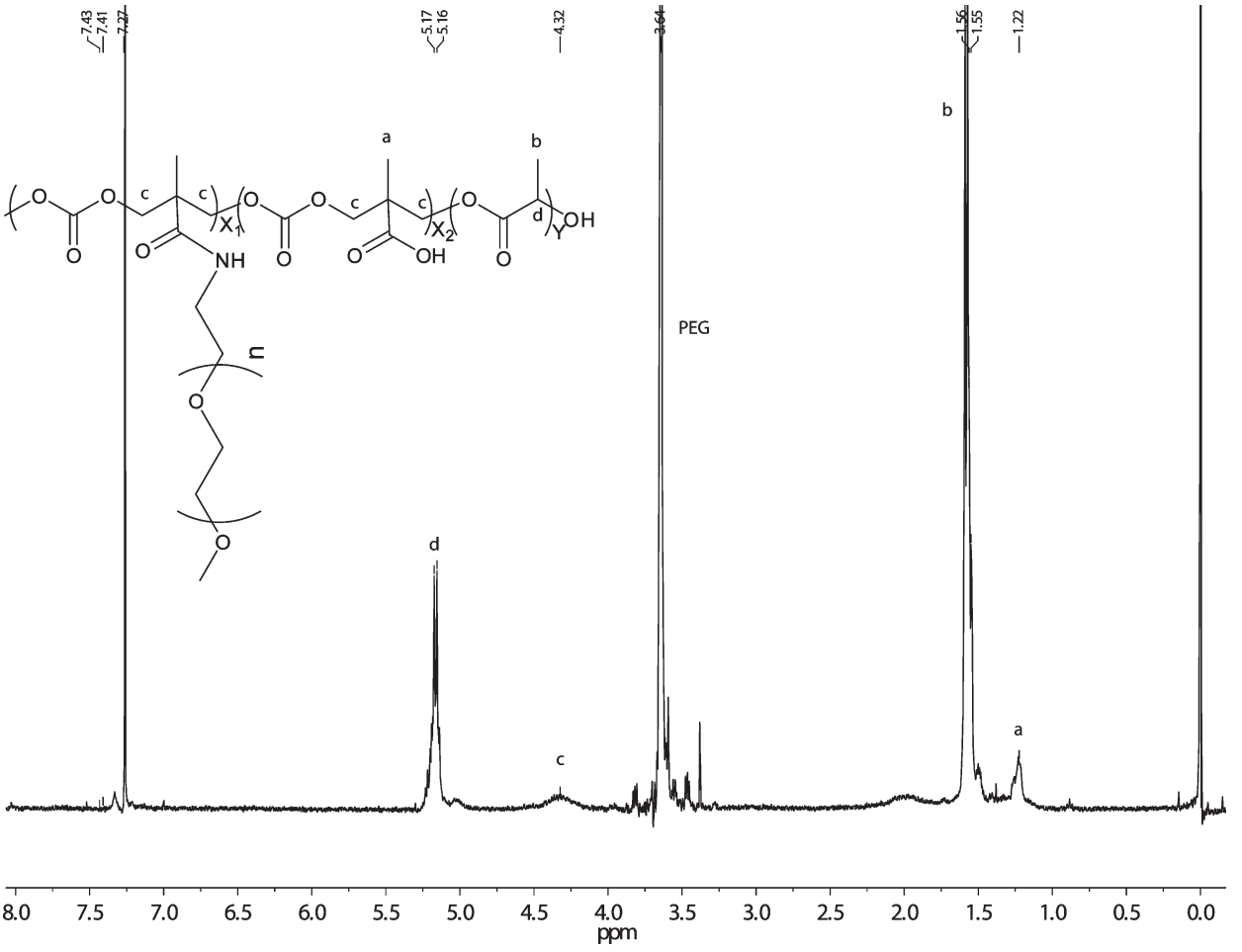

Figure 3. ^{1}H NMR spectrum of P(LA-*co*-TMCC)-*g*-PEG. ^{1}H NMR ($CDCl_3$): δ 1.23 (m, CH_3 from TMCC), 1.57−1.59 (m, CH_3 from LA), 3.64 (bs, PEG), 4.34 (m, methylene from TMCC), and 5.16 (m, CH from LA).

added, resulting in a borate buffer concentration of 16 mM. The resulting colloidal solution was placed in a dialysis bag and dialyzed against distilled water to remove DMF.

Copolymer Self-Assembly at pH 5 or 7 with 167 mM Borate Buffer. P(LA-*co*-TMCC)-*g*-PEG (4 mg) was dissolved in 1.0 mL of DMF, and then 0.5 mL of borate buffer (pH 5 or 7, 500 mM) was added, yielding a borate buffer concentration of 167 mM and a clear solution. The resulting colloidal solution was placed in a dialysis bag and dialyzed against distilled water to remove the DMF for 24 h. (This method cannot be used with pH 9 borate buffer because the sodium borate salt precipitates out of solution.)

Nanoparticle Stability Test. Nanoparticles were stored in water at 4 °C over a 4 month period. At the end of every month, nanoparticle size was measured by Zetasizer.

Results

Synthesis and Characterization of P(LA-*co*-TMCC-Bn) 5. P(LA-*co*-TMCC-Bn) **5** was synthesized by the ROP of D,L-LA and TMCC-Bn using pyrene butanol initiation and thiourea amine bifunctional organocatalysis. A series of copolymers was synthesized. For example, with a monomer feed ratio of 90 mol % LA and 10 mol % TMCC-Bn and a monomer-to-initiator ratio, [M]:[I] of 50, LA and TMCC-Bn were polymerized to P(LA-*co*-TMCC-Bn) with 99% conversion after 7 days (Table 1). The copolymer had a GPC-determined number-average molar mass, M_n of 6200 g/mol, a PDI of 1.25, and a degree of polymerization for LA, n_{LA}, of 77, and for TMCC-Bn, $n_{TMCC\text{-}Bn}$, of 7 based on ^{1}H NMR data. The molar concentration of TMCC-Bn in the copolymer was calculated at 8.3 mol %, which was lower than the monomer feed ratio of 10 mol %, yet is referred to in the subsequent text as 10 mol % TMCC in the copolymer.

As the monomer-to-initiator ratio doubled to [M]:[I] of 100, the number-average molar mass of P(LA-*co*-TMCC-Bn) with a feed monomer concentration of 10 mol % TMCC-Bn almost doubled to M_n of 11 800 g/mol. By varying the monomer feed ratio, copolymers with 20 and 35% TMCC-Bn were

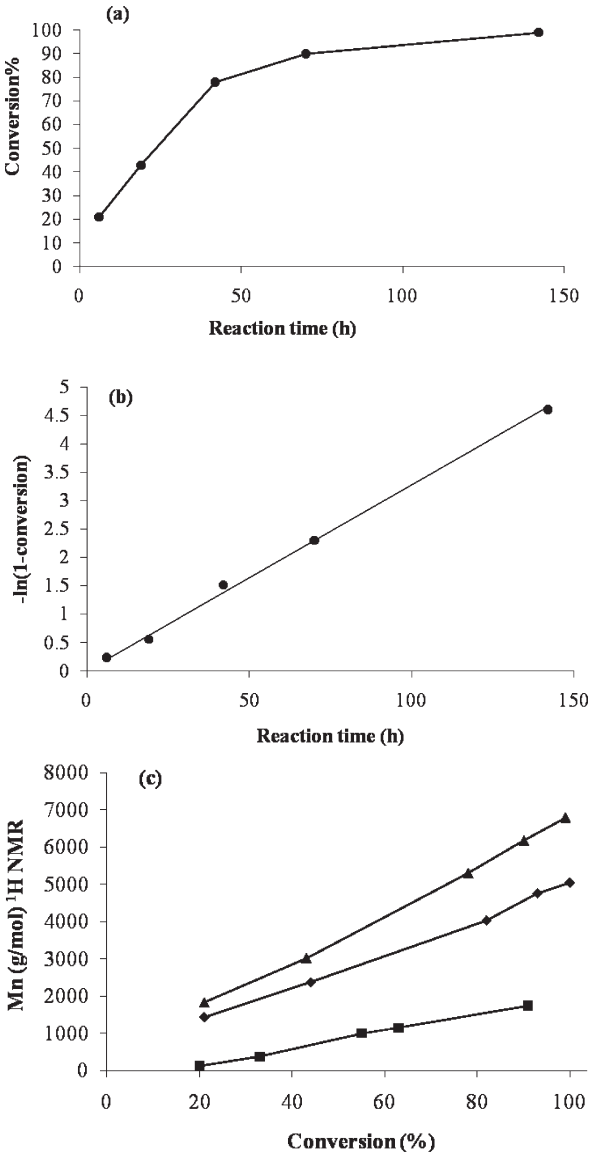

Figure 4. (a) Percent polymer conversion increases with reaction time; (b) plot of −ln(1-conversion) with reaction time demonstrates first-order kinetics; and (c) M_n (LA, ◆), M_n (TMCC-Bn, ■), and M_n (total, ▲) increases linearly with % monomer conversion to the copolymer, as estimated by ^{1}H NMR.

synthesized. A longer reaction time was required to achieve 95% conversion, yet the feed concentrations of TMCC-Bn were similar to those in the copolymers. The difference in percent conversion for 10 versus 20 and 30 mol % TMCC primarily reflects the lower conversion of TMCC (80−90%) relative to LA (98−100%) and the increased composition of TMCC in the copolymers.

The initiation efficiency was estimated from the ^{1}H NMR of the 10% TMCC copolymer. For [M]:[I] = 50, the initiator efficiency was estimated at 92%, based on the estimated DP of the copolymer of 46, which is similar to literature values for pure PLA, which is ~100%.[17]

To gain greater insight into the polymerization, a series of 1 mL samples, precipitated in 7 mL of hexane, were taken during the course of the 142 h copolymerization with 10 mol % TMCC-Bn at a [M]:[I] ratio of 50. The samples were characterized by ^{1}H NMR for both composition and percent conversion: the relative integrated peak areas of CH_2 from TMCC (4.32 ppm) and CH_3 from LA (1.57 to 1.59 ppm) to the conjugated pyrene (7.78 to 8.25 ppm) were used to calculate polymer composition, whereas the ratio of unreacted to polymerized monomers was used to calculate conversion. In Figure 4a, increased conversion with time is shown. To better understand the polymerization kinetics, a plot of −[ln(1-conversion)] versus time showed a linear relationship, thereby demonstrating first order kinetics. (Figure 4b). In Figure 4c, a linear increase in polymer molar mass with percent conversion is observed. This, together with the observation that PDI of the copolymer decreased from 2.9 to 1.3 as the polymerization proceeded (Figure 5), suggests that the polymerization is living. In this water-sensitive polymerization, water competes with the alcohol initiator for the thiourea-amine catalyst and terminates the polymerization, thereby complicating the formation of monodisperse polymer.

Reactivity Ratios of LA and TMCC-Bn. On the basis of the mole fraction feed composition, f_{LA}, and the mole fraction copolymer composition, F_{LA} (summarized in Table 2), the monomer reactivity ratios for LA and TMCC-Bn were calculated for $r_{(LA)}$ at 1.1 and $r_{(TMCC\text{-}Bn)}$ at 0.072. Figure 6a shows the ellipse calculated from the EVM method using the estimated error values.

Figure 6b shows a graphical presentation of the Mayo−Lewis equation for the instantaneous copolymer composition of PLA as a function of LA content in the monomer feed composition. The copolymer composition is more enriched with LA than with TMCC-Bn at all monomer feed ratios, indicating that both LA is consumed more rapidly than TMCC-Bn, and compositional drift likely occurs during the course of the polymerization. Because TMCC-Bn is much less reactive than LA, an increase in TMCC-Bn content decreases the rate of ring-opening copolymerization as well as lowers the total degree of polymerization (Table 1).

Self-Assembly of P(LA-*co*-TMCC)-*g*-PEG. Methoxy-terminated poly(ethylene glycol) amine (MeO-PEG-NH_2) with a molar mass of either 5 or 10 kg/mol was grafted to P(LA-*co*-TMCC) with 10, 20, or 35% TMCC using DIC chemistry. In the ^{1}H NMR spectrum of P(LA-*co*-TMCC)-*g*-PEG, the characteristic peak of PEG appeared at 3.64 ppm, confirming the successful grafting of PEG to the copolymer backbone (Figure 3). On the basis of the integrated peak areas at 4.34 (CH_2 from TMCC) and 3.64 ppm (CH_2 from PEG), it was estimated that there was one grafted PEG chain to every P(LA-*co*-TMCC) backbone.[19] In brief, the number of PEGs per copolymer backbone was calculated based on eq 2

$$\frac{n(\text{H on PEG}) \times n(\text{PEG})}{\text{DP}_{(\text{TMCC})} \times 3} = \frac{A_{(\text{PEG})}}{A_{\text{TMCC-methyl group}}} \qquad (2)$$

where $n_{(\text{H on PEG})}$ is the total number of protons per PEG chain; $n_{(\text{PEG})}$ is the number of PEG chains per copolymer backbone; $\text{DP}_{(\text{TMCC})}$ is the degree of polymerization of TMCC; $A_{(\text{PEG})}$ is the integral area of PEG protons from the ^{1}H NMR spectrum, and $A_{\text{TMCC-methyl group}}$ is the intergral area of methyl protons on TMCC.

Because P(LA-*co*-TMCC) is a random copolymer with likely enriched LA and TMCC repeats due to the disparity in monomer reactivity ratios, steric hindrance may limit grafting of additional PEG chains after the first chain is grafted. Consequently, the resulting P(LA-*co*-TMCC)-*g*-PEG has a hydrophobic P(LA-*co*-TMCC) backbone and a hydrophilic PEG pendant group, resulting in an amphiphilic polymer that self-assembles in aqueous environments.

The size, ζ potential and CMC of self-assembled polymeric nanoparticles depend on several factors including

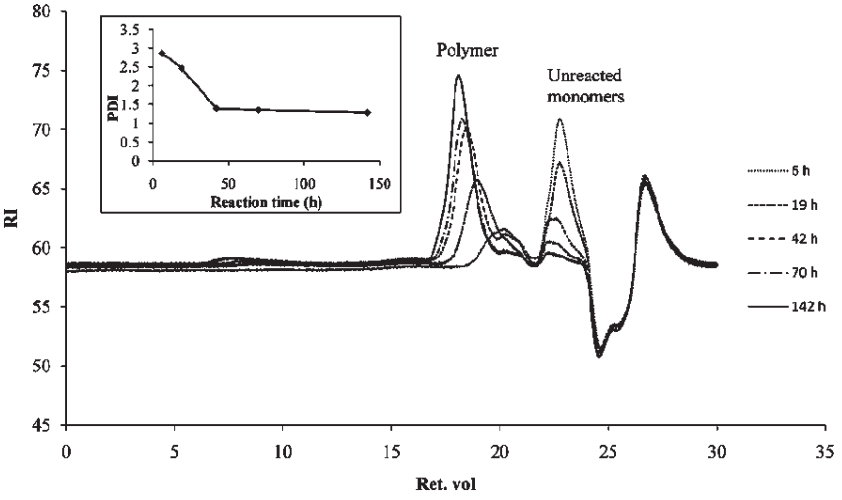

Figure 5. Evolution of gel permeation chromatogram for benzyl-protected P(LA-*co*-TMCC-Bn) obtained from ring-opening copolymerization at 6, 19, 42, 70, and 142 h. THF was the mobile phase. The peaks on the left are the copolymers formed, whereas the peaks on the right are predominantly unreacted monomers. The inset shows the decrease in copolymer PDI with increased polymerization time.

Table 2. Series of P(LA-*co*-TMCC-Bn) Were Synthesized at Low Conversion to Allow Reactivity Ratios to Be Calculated

% LA[a]	% TMCC-Bn[a]	copolymerization time (h)	% conversion[b]	% LA in copolymer[c]	% TMCC-Bn in copolymer[c]
45	10	5.0	7.4	45	11
35	30	6.0	9.9	38	25
25	50	5.5	8.7	33	34
15	70	5.5	9.2	30	40
5	90	5.5	9.0	20	60

[a] Monomer feed ratio. Each LA monomer contains two repeating units. [b] Determined by ^{1}H NMR measurement in $CDCl_3$. Calculated by comparing the integral signals from unreacted and polymerized monomers. [c] Determined by ^{1}H NMR measurements in $CDCl_3$. Calculated by comparing the integrated peak areas of the signals at δ 4.32 (CH_2, TMCC-Bn) with those measured at δ 1.35−1.55 (CH_3, LA).

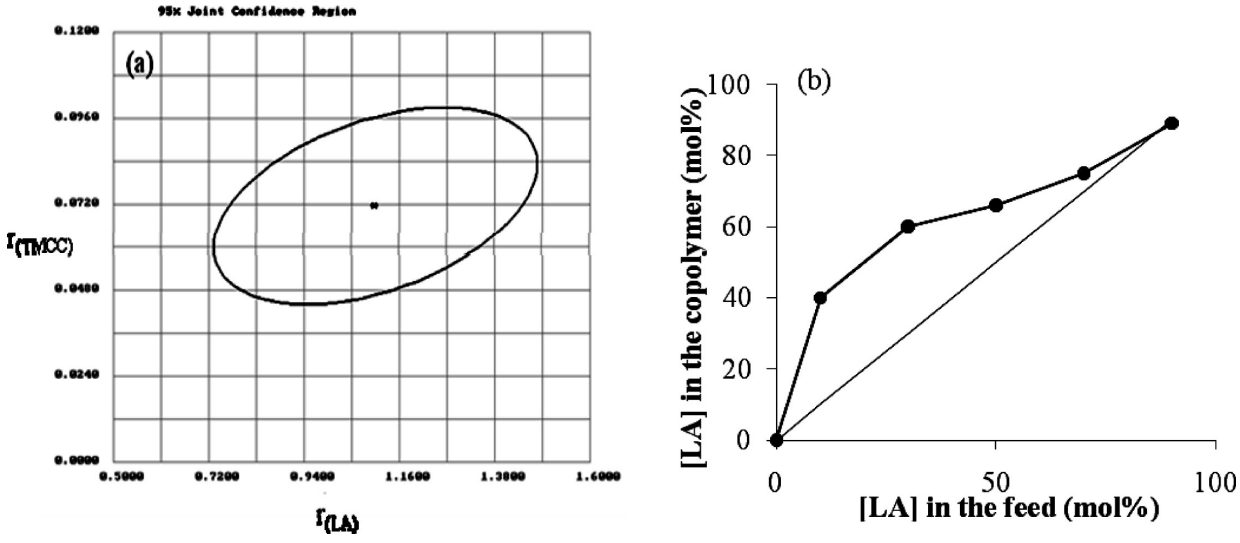

Figure 6. (a) Monomer reactivity ratios for $r_{(TMCC\text{-}Bn)}$ and $r_{(LA)}$ were calculated at 0.072 and 1.1, respectively, using the error-in-variables method and the RREVM software package. The elliptical shape on the graph shows the 95% posterior probability contour; (b) composition curve of P(LA-*co*-TMCC-Bn) where (●) represents LA. The straight line represents conditions when both monomers have the same reactivity ratio ($r_1 = r_2$).

copolymer composition, the hydrophobic to hydrophilic molar mass ratio, and pH of the borate buffer during dialysis processing.[25,26]

Copolymer Self-Assembly in Water versus in pH 9 Borate Buffer. Because P(LA-*co*-TMCC)-*g*-PEG is insoluble in water, self-assembled nanoparticles were prepared by dialysis. The copolymer was first dissolved in dimethyl formamide (DMF), which is miscible in water and a good solvent for both hydrophobic and hydrophilic blocks of P(LA-*co*-TMCC)-*g*-PEG. Then, either water or borate buffer solution was added gradually to decrease the quality of the solvent for the hydrophobic backbone, resulting in the self-assembly of hydrophobic P(LA-*co*-TMCC) in the core and hydrophilic PEG in the corona, exposed to water. The excess organic solvent was removed by dialysis.

The self-assembled nanoparticles prepared in water versus pH 9 borate buffer were compared for a series of compositions in terms of size and distribution (Figure 7). For all polymer

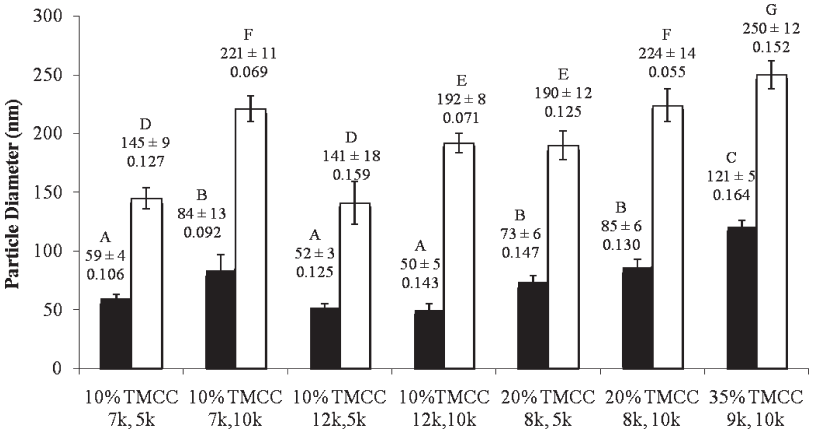

Figure 7. Particles self-assembled at pH 9 with 16 mM borate buffer (black bars) and in water (white bars). For each P(LA-*co*-TMCC)-*g*-PEG sample, the % TMCC in the copolymer is indicated, and the first number is the molar mass of the P(LA-*co*-TMCC), whereas the second number is the molar mass of the PEG grafted. For example, 10% TMCC 7K, 5K represents P(LA-*co*-TMCC) with 10% TMCC in the copolymer, having a backbone molar mass of 7 kg/mol and a PEG grafted molar mass of 5 kg/mol. The numbers above each bar are the mean particle diameter ± standard deviation (nm) and PDI measured by the Zetasizer ($n = 3$ independent tests). ANOVA was used for statistical analysis where different letters indicate significant differences ($p < 0.05$) according to the Newman−Keuls multiple comparison test.

compositions compared, nanoparticles self-assembled in pH 9 borate buffer were consistently (and significantly) smaller than those self-assembled in water. At pH 9, most of the TMCC carboxylic acids are deprotonated, resulting in repulsion among the P(LA-*co*-TMCC) chains. This limits the number of chains that can self-assemble into the nanoparticles, thereby constraining the diameter of the nanoparticles formed, and is consistent with previous reports.[18]

Unlike traditional amphiphilic block copolymers where the hydrophobic segments lack ionic or hydrophilic substitutes, our copolymers contain TMCC carboxylic acids. The presence of carboxylic acids impacts the thermodynamic stability of self-assembled nanoparticles. Interestingly, nanoparticle size increased with TMCC mol % in the copolymer whether self-assembled in water or pH 9 buffer (Figure 7). The increase in nanoparticle size was observed for copolymer compositions with: PEG 10K from 10% TMCC (12K, 10K) to 20% TMCC (8K, 10K) to 35% TMCC (9K, 10K) and PEG 5K from 10% TMCC (12K, 5K) to 20% TMCC (8K, 5K). As TMCC mol % increased, the LA mol % necessarily decreased (Table 1), resulting in a less hydrophobic backbone. To form stable nanoparticles based on hydrophobic interactions in the core, more polymer chains were required to self-assemble, thereby accounting for the increased size.

The stability of nanoparticles stored at 4 °C was tested over time using the 10% TMCC (12K, 5K) self-assembled nanoparticles processed with borate buffer (pH 9, 500 mM). Particle size was determined every month. We found that the nanoparticles were stable for at least 3 months, as indicated by a constant nanoparticle size at: time 0: 52 ± 3 nm, PDI = 0.110; 1 month: 53 ± 1 nm, PDI = 0.113; 2 months: 52 ± 4 nm, PDI = 0.130; and 3 months (49 ± 3 nm, PDI = 0.110).

Particle Self-Assembly As a Function of pH. To understand the effect of pH on self-assembly, P(LA-*co*-TMCC)-*g*-PEG having 10 mol % TMCC, a backbone molar mass of 12 kg/mol, and a PEG molar mass of 5 kg/mol was self-assembled in the presence of borate buffer (16 mM vs 167 mM) at pH 5, 7, or 9, the data of which are summarized in Figure 8. The pH of the borate buffer had a significant effect on nanoparticle size, whereas the concentration of borate buffer did not. As pH decreased from pH 9 to 7 to 5, P(LA-*co*-TMCC) carboxylate anions became protonated, resulting in nanoparticles with greater diameters likely because more chains self-assembled into the nanoparticles because of the decreased

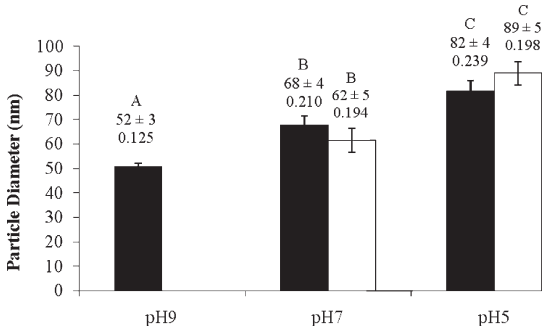

Figure 8. Self-assembled nanoparticle diameter as a function of pH with a final borate buffer concentration of 16 (black) and 167 mM (white) prepared from P(LA-*co*-TMCC)-*g*-PEG with 10 mol % TMCC, 12 kg/mol P(LA-*co*-TMCC), and 5 kg/mol PEG. Shown are the mean ± standard deviation for $n = 3$ independent tests. One-way ANOVA was used for statistical analysis. The Newman−Keuls multiple comparison test showed that there is a statistical difference ($p < 0.05$) between the different letters. Note that at the higher 167 mM borate buffer concentration at pH 9, the sodium borate salt precipitates out of the solution prohibiting nanoparticle formation.

repulsion of TMCC carboxylate ions; however, the nanoparticle distribution also increased with the decreased pH, suggesting some aggregation at pH 5. The slightly charged core of nanoparticles synthesized at pH 9 may prevent their aggregation. This is consistent with DLVO theory,[27] where electrostatic repulsion between small colloidal particles with the same charge results in stable particles.

Interestingly, the presence of buffer resulted in smaller nanoparticles. For example, nanoparticles self-assembled in water had a diameter of 141 ± 18 nm (Figure 7, 10% TMCC 12k, 5k) whereas those self-assembled in pH 7 borate buffer had a diameter of 68 ± 4 nm (at 16 mM borate buffer) and 62 ± 5 (at 167 mM borate buffer, Figure 8). The decreased nanoparticle size observed in the pH 7 borate buffer (relative to pH 7 water) likely results from borate anions lowering the interfacial free energy between nanoparticles and aqueous solutions.

ζ Potential and Critical Micelle Concentration. The ζ potential of each nanoparticle solution was measured at 1 mg/mL in water. Because the polymer backbone comprises carboxylate functional groups, the nanoparticle core has a negative charge and a negative ζ potential value (Figure 9a).

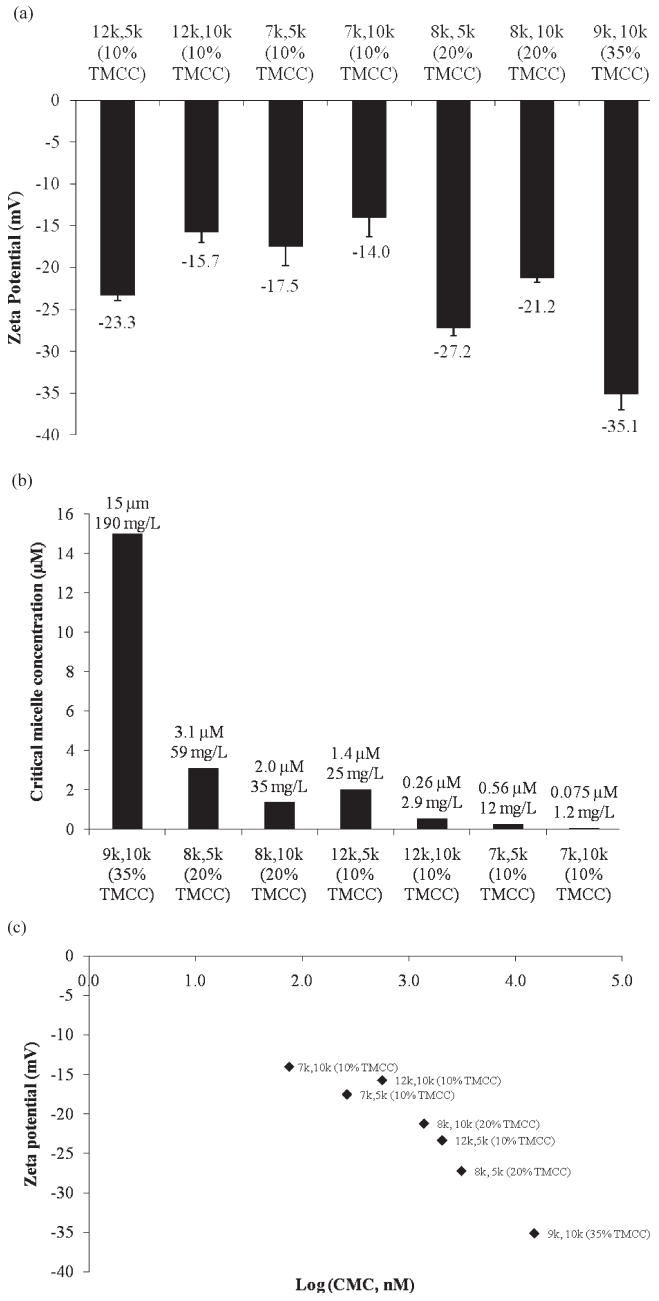

Figure 9. Particles were self-assembled at pH 9 with 16 mM of borate buffer. (a) ζ potential measurement of nanoparticles in water at 1 mg/mL; (b) CMC of nanoparticles in 10 mM PBS at pH 7.4, as determined by Whilhelmy balance; (c) correlation between ζ potential and CMC.

Several trends were observed. The negative ζ potential increased with TMCC content at a given PEG molar mass: for PEG 5 kg/mol, the negative ζ potential increased from −17.5 to −27.2 mV for P(LA-*co*-TMCC) with 10 and 20% TMCC, respectively; similarly for PEG 10 kg/mol, the negative ζ potential increased from −14.0 to −27.2 to −35.1 mV for P(LA-*co*-TMCC) with 10, 20, and 35% TMCC, respectively. Moreover, at a given TMCC concentration, a decrease in the negative ζ potential was observed as PEG molar mass increased as exemplified at: 10% TMCC 12K, 5K (−23.3 mV) versus 12K, 10K (−15.7 mV); 10% TMCC 7K, 5K (−17.5 mV) versus 7K, 10K (−14.0 mV); and 20% TMCC 8K, 5K (−27.2 mV) versus 8K, 10K (−21.2 mV). This suggests that the longer PEG chains in the corona more effectively shield the core TMCC carboxylate groups in the backbone from water than the shorter PEG chains.

The CMC of the nanoparticles was measured using the Wilhelmy plate method, as previously described[28,29] using a Sigma 700 tensiometer (Figure 9b). As the percent TMCC increased, the CMC increased, suggesting that the nanoparticles are more likely to disassemble upon dilution with greater charge (and hydrophilicity) in the core. For example, for P(LA-*co*-TMCC)-*g*-PEG with 10 kg/mol PEG, the CMC increased from 0.075 μM (1.2 mg/L) for 10% TMCC to 1.4 μM (25 mg/L) for 20% TMCC to 15 μM (190 mg/L) for 35% TMCC. Even at 10% TMCC, the CMC increased with an increase in the backbone from 0.075 μM (1.2 mg/mL) for the 7 kg/mol backbone to 0.56 μM (12 mg/L) for the 12 kg/mol backbone. Furthermore, the 35% TMCC nanoparticles with 10 kg/mol PEG were recovered at only 10% yield, whereas those with 5 kg/mol PEG were unrecoverable. This suggests that the TMCC carboxylate groups significantly destabilize the core resulting in a high CMC.

The ratio of hydrophilic to hydrophobic chain length also affected the CMC. For a given TMCC composition, as the molar mass ratio of PEG to P(LA-*co*-TMCC) increased, the CMC decreased, demonstrating more thermodynamically stable nanoparticles. For example, at 10 mol % TMCC, the nanoparticles had the lowest CMC at the PEG-to-backbone molar mass ratio of 10K:7K (0.075 μM or 1.2 mg/L), followed by 5K:7K (0.26 μM or 12 mg/L) and then 5K:12K (2.0 μM or 35 mg/L). A similar trend was observed for 20 mol % TMCC. Because the PEG corona shields the P(LA-*co*-TMCC) from water, the longer the PEG chain relative to the backbone, the more effective this shielding and the lower the CMC. In Figure 9c, a correlation of ζ potential and CMC shows a general trend that nanoparticles having a more negative ζ potential correspond to higher CMC values and thus less thermodynamically stable self-assembled nanoparticles.

To complement our understanding of the P(LA-*co*-TMCC)-*g*-PEG nanoparticle structure, the nanoparticles were imaged by TEM. As shown by the representative images in Figure 10, the nanoparticles appear to have a spherical structure. The mean diameter (±standard deviation) of the nanoparticles was measured at 54 ± 9 nm (n = 100 nanoparticles), which is similar to the size measured by dynamic light scattering of 52 ± 3 nm (shown in Figure 8). The nanoparticles imaged were prepared in water of P(LA-*co*-TMCC)-*g*-PEG having 10 mol % TMCC, 12 kg/mol backbone, and 5 kg/mol PEG.

Discussion

ROP using organocatalysts has been advanced in the past few years by Hedrick et al.[17,30−33] for the synthesis of several polymers including poly(ε-caprolactone), poly(carbosiloxane), poly(lactide), and PTMC with controlled molar mass and low PDI. We advanced this living ROP methodology in the synthesis of P(LA-*co*-TMCC), demonstrating the first example of a random copolymer of D,L-LA and TMCC using thiourea-amine organocatalysis with pyrene butanol initiation. This bifunctional catalyst brings the monomer and initiator close together through H-bonding interactions between carbonyl and alcohol functional groups, likely accounting for the living nature of the copolymerization. Importantly, the thiourea catalyst residues can be easily removed using chromatography, thereby eliminating any potential cytotoxicity associated with unreacted initiator. This is in contrast with standard synthetic methods of PLA and PTMCC where metal catalysts, such as Sn, are difficult to remove and known to be cytotoxic, even at low levels.

The PDI of P(LA-*co*-TMCC) synthesized by thiourea amine organocatalysis with pyrene butanol initiation was significantly

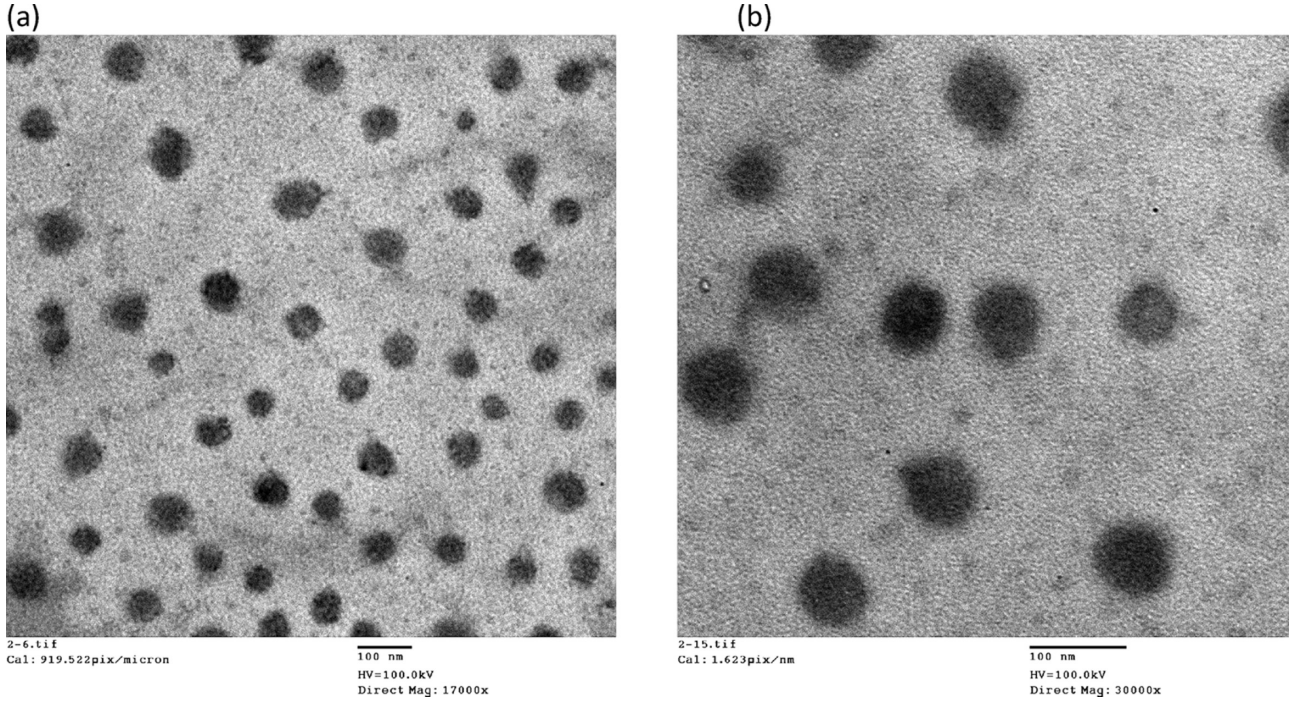

Figure 10. Representative TEM images of P(LA-*co*-TMCC)-g-PEG nanoparticles prepared in pH 9 borate buffer (16 mM) with 10 mol % TMCC, 12 kg/mol backbone, and 5 kg/mol PEG at: (a) low and (b) high magnification (scale bar is 100 nm in both images). The mean (and standard deviation) diameter of the nanoparticles is 54 ± 9 nm (n = 100 nanoparticles).

narrower (between 1.25 and 1.36) than that previously synthesized by stannous octanoate melt polymerization (between 2.30 and 2.70).[18,19] Moreover, comparing copolymers with 10 mol % TMCC, the self-assembled nanoparticles of P(LA-*co*-TMCC)-*g*-PEG formed from the near monodisperse polymer had a narrower population distribution (0.092 to 0.14) than those formed from the polydisperse polymer (0.21 to 0.29), thereby proving our hypothesis. Having a narrow population distribution of polymeric nanoparticles is desirable for applications in drug delivery because the encapsulation efficiency and drug loading will be more uniform across the nanoparticles, which directly impacts the drug release profile.[25] Furthermore, in cancer applications, nanoparticle size is critical to its ability to cross the hyperpermeabilized vascularature of many tumors.[1]

A key driving force in nanoparticle self-assembly is the minimization of the interfacial free energy. The interfacial free energy is governed by the balance of forces between van der Waals interactions among the hydrophobic groups and opposing hydration of the hydrophilic chain.[34] In this study, the factors that influence the interfacial free energy include the addition of borate buffer (salt effect), change of pH (acid effect), and the percentage of LA in P(LA-*co*-TMCC) (hydrophobic effect). During the nanoparticle self-assembly, hydrophilic PEG chains present in the corona are hydrated by water through hydrogen bonding interactions between the ether oxygen and the water molecules.[35] The presence of borate anions disrupts the hydrogen bonding between PEG and water, thereby dehydrating the PEG chain.[35] The repulsion due to hydration of PEG chains is thus reduced; therefore, the interfacial tension is also reduced. This results in smaller nanoparticles (Figure 7). As the pH decreases in the system from pH 9 to 5 (Figure 8), the ether oxygens on PEG likely become protonated, forming oxonium ions.[36] Consequently, repulsion between the PEG chains increases, resulting in larger nanoparticles.[35]

Nanoparticles that are self-assembled from amphiphilic copolymers containing polar monomer repeat units in the hydrophobic segment are rarely studied yet provide another mechanism to control nanoparticle size. At pH 9, most of the carboxylic acids are deprotonated and increase the repulsion among the hydrophobic groups. Therefore, less polymer self-assembles to form micelles, resulting in smaller nanoparticles.

Consistent with minimization of the interfacial free energy being a driving force for self-assembly, P(LA-*co*-TMCC)-*g*-PEG nanoparticles increased in size with increased TMCC composition (Figure 7). Here the polar headgroup is composed of primarily PEG, yet TMCC carboxylates expand the headgroup surface area, whereas the length of hydrophobic group (mostly composed of LA) decreases. This leads to an increase in interfacial tension as reflected in the higher CMC data. The size of the nanoparticles increases to accommodate the larger surface area of the hydrophilic headgroup.

The living polymer synthesis that was used to synthesize P(LA-*co*-TMCC)-*g*-PEG allowed us to manipulate polymer composition, molar mass, and distribution, which influenced nanoparticle size, distribution, and CMC. The CMC is critical in drug delivery applications where the stability of the polymeric nanoparticle affects the success of releasing encapsulated drugs at the desired tissue site. Typically, in cancer, nanoparticle formulations are injected intravenously, where there is an immediate dilution in blood. It is for this reason that CMC is a key feature in nanoparticle systems.

The CMC of an amphiphilic copolymer is influenced by many factors, such as the nature and the length of the core-forming block, length of the hydrophilic block, and presence of a surfactant.[25] The hydrophobicity of the hydrophobic block impacts the CMC where the more hydrophobic the block, the lower the CMC in water.[25] For example, the CMC values for PS-*b*-PEO copolymers range between 1 and 5 mg/L,[37] whereas a PLA-*b*-PEO system has a CMC of 35 mg/L.[29] In our system, the CMC range was from 1.2 to 190 mg/L, where the higher CMC corresponded to those nanoparticles formed from polymers having 35 mol % TMCC. The most stable nanoparticles (with a CMC of 1.2 mg/L) had 10 mol % TMCC in the backbone and higher molar mass ratio of PEG to P(LA-*co*-TMCC).

For most amphiphilic copolymers, increasing the molar mass of the core-forming hydrophobic block while keeping the corona-forming hydrophilic block constant results in a decreased CMC (i.e., more stable nanoparticles).[38,39] In our system, however, the CMC increased as the hydrophobic chain length increased from 7 to 12 kg/mol at constant PEG molar mass for P(LA-*co*-TMCC)-*g*-PEG with 10% TMCC. With the increase in the hydrophobic chain length, the number of TMCC carboxylates also increased, resulting in a relatively less hydrophobic backbone. The higher CMC with increased P(LA-*co*-TMCC) molar mass was observed with both 5 and 10 kg/mol PEG grafts. The increased TMCC carboxylate concentration was reflected in the ζ potential measurements, which were more negative for 12 versus 7 kg/mol backbone regardless of molar mass of the PEG graft. The effect was significant at 5 kg/mol PEG. By increasing PEG molar mass from 5 to 10 kg/mol and keeping polymer backbone composition constant, the self-assembled nanoparticles were more stable, as reflected by a decreased CMC. The longer PEG chains more effectively shield the TMCC carboxylate charged groups, resulting in this decreased CMC.

The inclusion of PEG in the nanoparticle design was important to the self-assembly process and also to the ultimate application in drug delivery, where PEG modification promotes longer blood circulation times by decreasing protein adsorption and phagocytosis by macrophages, among other cell types.[40] Whereas high concentrations of TMCC significantly decreased the nanoparticle stability, as reflected in higher CMCs, lower concentrations of TMCC resulted in acceptable CMC values and at the same time provide a means to graft PEG (as shown herein) and other molecules, such as fluorophores for imaging purposes. With a CMC of 0.075 μM, these amphiphilic polymeric nanoparticles can be diluted to a concentration of 75 nM before disassembling. For example, given that the blood volume in a mouse is ~1.5 to 2 mL and the maximum injected volume is 200 μL, a 10-fold dilution of the nanoparticles will occur upon injection. This suggests that nanoparticles injected at a concentration >0.75 μM (12 mg/L) will be stable; however, we acknowledge that blood−protein interactions may further destabilize the nanoparticles, albeit through a different mechanism, which forms the basis of future studies.

Conclusions

P(LA-*co*-TMCC-Bn) was successfully synthesized with pyrene butanol initiation and thiourea amine organocatalysis with different molar masses and percentages of TMCC-Bn. A linear increase in polymer molar mass versus percent conversion as well as a decrease in PDI indicated a living copolymerization. The monomer reactivity ratios, estimated by the EVM method, demonstrated that LA is 15 times more reactive than TMCC-Bn. The P(LA-*co*-TMCC) grafted with PEG resulted in an amphiphilic polymer that self-assembled in aqueous solution to form nanoparticles. By controlling the pH and the copolymer composition, the nanoparticle size, ζ potential, and CMC were tuned. The TEM data confirmed the DLS results of nanoparticle diameter and narrow size distribution resulting from near monodisperse polymer. In ongoing studies, the nanoparticles are being studied for targeted drug delivery applications in cancer, where size and composition will influence blood circulation time and biodistribution.

Acknowledgment. We thank Professor Mark Taylor for advice on polymer synthesis; Dr. Shawn Owen for insight into the driving forces for self-assembly; Professor Warren Chan for use of his Zetasizer; Professor Edgar Acosta for use of his Wilhelmy plate; and Professor Mitchell Winnik and Daniel Majonis for use of their GPC. We are grateful for funding from the Ontario Centers of Excellence, C.M.M. for the Champions of Research program (M.S.S.), and the Ontario Graduate Studentships in Science and Technology (J.L.).

References and Notes

(1) Maeda, H. *Adv. Enzyme Regul.* **2001**, *41*, 189–207.
(2) Allen, T. M.; Cullis, P. R. *Science* **2004**, *303*, 1818–1822.
(3) Duncan, R. *Nat. Rev. Drug Discovery* **2003**, *2*, 347–360.
(4) Bala, I.; Hariharan, S.; Kumar, M. N. *Crit. Rev. Ther. Drug Carrier Syst.* **2004**, *21*, 387–422.
(5) Jerome, C.; Lecomte, P. *Adv. Drug Delivery Rev.* **2008**, *60*, 1056–1076.
(6) Albertsson, A. C.; Varma, I. K. *Biomacromolecules* **2003**, *4*, 1466–1486.
(7) Pego, A. P.; Poot, A. A.; Grijpma, D. W.; Feijen, J. *J. Biomater. Sci., Polym. Ed.* **2001**, *12*, 35–53.
(8) Dechy-Cabaret, O.; Martin-Vaca, B.; Bourissou, D. *Chem. Rev.* **2004**, *104*, 6147–6176.
(9) Kamber, N. E.; Jeong, W.; Waymouth, R. M.; Pratt, R. C.; Lohmeijer, B. G. G.; Hedrick, J. L. *Chem. Rev.* **2007**, *107*, 5813–5840.
(10) Mullen, B. D.; Tang, C. N.; Storey, R. F. *J. Polym. Sci., Part A: Polym. Chem.* **2003**, *41*, 1978–1991.
(11) Zhang, X. J.; Mei, H. J.; Hu, C.; Zhong, Z. L.; Zhuo, R. X. *Macromolecules* **2009**, *42*, 1010–1016.
(12) Storey, R. F.; Mullen, B. D.; Melchert, K. M. *J. Macromol. Sci., Pure Appl. Chem.* **2001**, *38*, 897–917.
(13) Shi, M.; Wosnick, J. H.; Ho, K.; Keating, A.; Shoichet, M. S. *Angew. Chem., Int. Ed.* **2007**, *46*, 6126–6131.
(14) Okino, T.; Hoashi, Y.; Takemoto, Y. *J. Am. Chem. Soc.* **2003**, *125*, 12672–12673.
(15) Okino, T.; Nakamura, S.; Furukawa, T.; Takemoto, Y. *Org. Lett.* **2004**, *6*, 625–627.
(16) Hoashi, Y.; Okino, T.; Takemoto, Y. *Angew. Chem., Int. Ed.* **2005**, *44*, 4032–4035.
(17) Dove, A. P.; Pratt, R. C.; Lohmeijer, B. G.; Waymouth, R. M.; Hedrick, J. L. *J. Am. Chem. Soc.* **2005**, *127*, 13798–13799.
(18) Shi, M.; Shoichet, M. S. *J. Biomater. Sci., Polym. Ed.* **2008**, *19*, 1143–1157.
(19) Lu, J.; Shi, M.; Shoichet, M. S. *Bioconjugate Chem.* **2009**, *20*, 87–94.
(20) Gohy, J. F. *Adv. Polym. Sci.* **2005**, *190*, 65–136.
(21) Han, J. N.; Pyun, S. I.; Yang, T. H. *J. Electrochem. Soc.* **1997**, *144*, 4266–4272.
(22) Reilly, P. M.; Patinoleal, H. *Technometrics* **1981**, *23*, 221–231.
(23) Dube, M.; Sanayei, R. A.; Penlidis, A.; Odriscoll, K. F.; Reilly, P. M. *J. Polym. Sci., Part A: Polym. Chem.* **1991**, *29*, 703–708.
(24) Jie, C.; Zhu, K. J. *Polym. Int.* **1997**, *42*, 373–379.
(25) Allen, C.; Maysinger, D.; Eisenberg, A. *Colloids Surf., B* **1999**, *16*, 3–27.
(26) Cheng, J.; Teply, B. A.; Sherifi, I.; Sung, J.; Luther, G.; Gu, F. X.; Levy-Nissenbaum, E.; Radovic-Moreno, A. F.; Langer, R.; Farokhzad, O. C. *Biomaterials* **2007**, *28*, 869–876.
(27) Verwey, E. J. W.; Overbeek, J. T. G. *Theory of the Stability of Lyophobic Colloids*; Elsevier: New York, 1948.
(28) Wan, L. S. C.; Lee, P. F. S. *J. Pharm. Sci.* **1974**, *63*, 136–137.
(29) Hagan, S. A.; Coombes, A. G. A.; Garnett, M. C.; Dunn, S. E.; Davis, M. C.; Illum, L.; Davis, S. S.; Harding, S. E.; Purkiss, S.; Gellert, P. R. *Langmuir* **1996**, *12*, 2153–2161.
(30) Connor, E. F.; Nyce, G. W.; Myers, M.; Mock, A.; Hedrick, J. L. *J. Am. Chem. Soc.* **2002**, *124*, 914–915.
(31) Lohmeijer, B. G. G.; Dubois, G.; Leibfarth, F.; Pratt, R. C.; Nederberg, F.; Nelson, A.; Waymouth, R. M.; Wade, C.; Hedrick, J. L. *Org. Lett.* **2006**, *8*, 4683–4686.
(32) Nederberg, F.; Lohmeijer, B. G. G.; Leibfarth, F.; Pratt, R. C.; Choi, J.; Dove, A. P.; Waymouth, R. M.; Hedrick, J. L. *Biomacromolecules* **2007**, *8*, 153–160.
(33) Nederberg, F.; Appel, E.; Tan, J. P.; Kim, S. H.; Fukushima, K.; Sly, J.; Miller, R. D.; Waymouth, R. M.; Yang, Y. Y.; Hedrick, J. L. *Biomacromolecules* **2009**, *10*, 1460–1468.
(34) Israelachvili, F. *Intermolecular and Surface Forces: With Applications to Colloidal and Biological Systems*; Academic Press: Great Britain, 1989.
(35) Malik, W. U.; Jhamb, O. P. *Kolloid Z. Z. Polym.* **1970**, *242*, 1209–1211.
(36) Hsiao, L.; Dunning, H. N.; Lorenz, P. B. *J. Phys. Chem.* **1956**, *60*, 657–660.
(37) Wilhelm, M.; Zhao, C. L.; Wang, Y. C.; Xu, R. L.; Winnik, M. A.; Mura, J. L.; Riess, G.; Croucher, M. D. *Macromolecules* **1991**, *24*, 1033–1040.
(38) Astafieva, I.; Zhong, X. F.; Eisenberg, A. *Macromolecules* **1993**, *26*, 7339–7352.
(39) Astafieva, I.; Khougaz, K.; Eisenberg, A. *Macromolecules* **1995**, *28*, 7127–7134.
(40) van Vlerken, L. E.; Vyas, T. K.; Amiji, M. M. *Pharm. Res.* **2007**, *24*, 1405–1414.